Journal of Electronic Materials, Vol. 12, No. 4, 1983

LPE GROWTH OF HIGH PURITY InP AND N- AND P-$In_{0.53}Ga_{0.47}As$

E. Kuphal and D. Fritzsche

Forschungsinstitut der Deutschen Bundespost
beim FTZ

D-6100 Darmstadt, Fed. Rep. of Germany

(Received December 14, 1982)

InP and $In_{0.53}Ga_{0.47}As$ layers on (100)-oriented InP substrates were grown by LPE having net carrier concentrations in the 10^{14} cm^{-3} range and 77 K electron mobilities of 75,000 and 53,000 $cm^2V^{-1}s^{-1}$, respectively. A bake scheme to purify the source materials was established which is very effective and time saving. The growth temperature T_G was decreased below 600 ^oC without loss of layer purity. The advantages of a low T_G are discussed. Mobility versus electron concentration curves are given and compared with published theoretical and experimental results. For the demands of inversion MISFET's, p-InGaAs has been grown for the first time with hole concentrations down to 5.5×10^{15} cm^{-3} by applying a novel doping technique. The distribution coefficient of Zn in InGaAs is found to be $k_{Zn} = 0.65 \pm 0.07$.

Key words: InP, $In_{0.53}Ga_{0.47}As$, liquid phase epitaxy, Hall mobility, distribution coefficient.

0361-5235/83/1204-0743$3.00 © 1983 AIME

Introduction

The efforts to grow high purity $In_{1-x}Ga_xAs_yP_{1-y}$ alloys lattice-matched to InP are stimulated by the demands of at least two device applications: Photodiodes for the 1.3 to 1.65 μm wavelength range and high speed inversion MISFET's. For InGaAs pin photodiodes a net carrier concentration of ~ 10^{15} cm^{-3} is required to obtain low-dark-current, low-capacitance devices operated at low voltage /1/. Recently, InGaAs pin diodes made of liquid phase epitaxial (LPE) material have been realized showing a dark current density as low as 0.9 x 10^{-5} A/cm^2 and C = 0.3 pF at - 10 V /2/. For n-channel inversion MISFET's a high field effect mobility μ_{FE} demands a low hole concentration in the channel layer. A low hole concentration, however, is only achieved, if the residual carrier concentration, which is always n-type in the InGaPAs system, is still lower. Recent results for InGaAs MISFET's are μ_{FE} = 725 cm^2/Vs for p = 2 x 10^{17} cm^{-3} /3/, but μ_{FE} = 2500 cm^2/Vs for p = 5.5 x 10^{15} cm^{-3} /4/.

In a previous study /5/ we have obtained layers with net electron concentrations below 10^{15} cm^{-3} over the entire range of the InGaAsP/InP system for seven different compositions. The room temperature (RT) mobilities of the purest layers were found to increase monotonically between InP and $In_{0.53}Ga_{0.47}As$, while the 77 K mobility reveals a minimum near y = 0.7 caused by alloy scattering and the miscibility gap. The alloy scattering limited mobility μ_{alloy} as a function of y was found to be considerably larger than reported earlier.

Meanwhile a trend is visible to move from InGaAsP to InGaAs as a starting material for photodetectors and FET's. One reason for this is that dark current densities in InGaAsP photodiodes are generally not smaller than in InGaAs photodiodes /1/ contrary to what would be

expected from the larger bandgap of InGaAsP. For FET's the higher electron mobility of the ternary compared to the quaternary is a strong incentive for its use. Therefore, we confine ourselves in this study to the endpoints InP and $In_{0.53}Ga_{0.47}As$ of the InGaAsP system. In the following, new results exceeding our previous work /5/ are presented. A new bakeout scheme for the source materials has been established, which is time saving. The growth temperature dependence of the purity of InP has been studied, and the advantages of a low growth temperature will be discussed. Mobility versus carrier concentration curves are presented for n-type InP and InGaAs. Furthermore, in order to grow p-InGaAs for MISFET's a novel doping technique using Zn-doped GaAs as a doping source is described, which allows very reproducible doping in the range 5.5×10^{15} cm^{-3} $\leq N_A - N_D \leq 1.5 \times 10^{18}$ cm^{-3}. Layer characterization was done by van der Pauw, C-V, x-ray diffraction and photoluminescence measurements.

The LPE growth system

Three liquid phase epitaxial (LPE) growth systems of identical design /5/ are used, in which more than 800 InP-based LPE structures have been grown so far. The horizontal multiple-bin sliding boat is machined of uncoated pure graphite, which we have purified in a RF furnace at 1400 °C in high-vacuum. After each loading, the LPE system is evacuated by a turbomolecular pump down to 1 x 10^{-5} mbar, and is then flushed with Pd-diffused hydrogen. The contamination of the H_2 gas is measured at the inlet and at the outlet of the epitaxial tube by H_2O monitors (Endress and Hauser, Maulburg) and at the outlet by an O_2 monitor (Research Inc., Minneapolis). The detection limits of these monitors are 0.1 ppm_v H_2O and 0.01 ppm_v O_2, respectively.

The substrate area used has been increased from 8 x 12 mm^2 to 15 x 20 mm^2. The larger epitaxial layers show less thickness inhomo-

geneity than the smaller layers did. Wipe-off of the solution causes no problems even for the large substrate size. Fig. 1 shows a micrograph of an $In_{0.53}Ga_{0.47}As$ layer with InP buffer layer. Its surface is seen to be macroscopically featureless.

Bakeout of the growth solution

It is well known that the residual impurity of LPE InP can be effectively reduced by an extended bake of the solution in flowing H_2. Various authors have baked the solution under H_2 containing traces of H_2O /6-8/, thus improving their layer purity. The Si impurity in the indium is believed to be oxidized to SiO_2 and no longer incorporated as a donor in InP. Another study states that addition of H_2O makes the results worse /9/. A wet H_2 atmosphere, however,

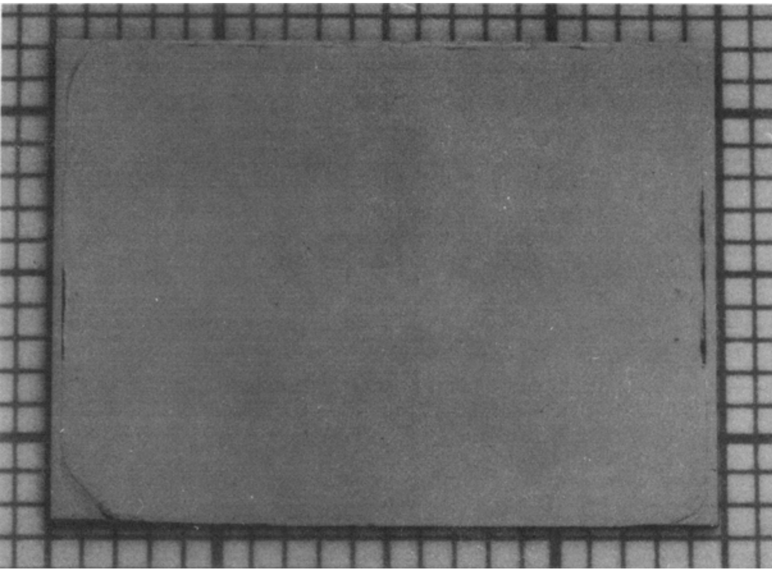

Fig. 1. Micrograph of an $In_{0.53}Ga_{0.47}As$ layer shown on a millimeter background. The layer was grown at 595 ^{o}C without a meltback step.

is principally undesired in LPE, since the surface of the solution may be oxidized and since oxygen induces a deep trap in InP /10/. Furthermore, the decomposition of the substrate under wet H_2 is enhanced.

To avoid these disadvantages, the following bakeout procedure was applied here: The indium (six 9's purity, from MCP) is baked in high-vacuum in a special furnace used only for this purpose, which contains a graphite boat designed for 100 g of In. The quartz tube is evacuated by a turbo-molecular pump to 2×10^{-6} mbar. A bake at 650 $^{\circ}$C for 50 h has proved to be very effective and to be better than an even longer bake in H_2. In this process volatile impurities such as S, Se, Te, Zn, Mg and Cd are evaporated from the In, whereas Si cannot be evaporated because of its small vapor pressure. The complete In + InP solution is then baked in the epitaxial tube without substrate under H_2 as dry as possible for not more than 15 h at 660 $^{\circ}$C. In this step essentially the source InP, which has an initial electron concentration of 4×10^{15} cm^{-3}, is purified. The solution is oversaturated making allowance for the evaporation loss of P from the uncapped solution. The amount of P evaporated under floating H_2 was calculated /11/. Since our long-term vacuum bake does not take place in the epitaxial tube, this bake scheme is considered to be very time saving. Using this procedure we have obtained comparable or even better electrical results (see following section) than those authors who added traces of H_2O and applied longer bake times /6-8/.

The raw In contains 0.1 ppm$_w$ Si according to the manufacturer's analysis, which would cause a donor concentration of ~ 10^{17} cm^{-3} in LPE InP. As we measure donor concentrations of only $\lesssim 10^{15}$ cm^{-3}, there must be a mechanism, which removes the Si. As mentioned above, wet H_2 lowers the Si equilibrium level. Although we did not intentionally add H_2O to the hydrogen, there are four effects which may act as unin-

tentional sources of H_2O or O_2. (I) The downstream cold part of the quartz tube generally contains a phosphorus deposition among which is hygroscopic P_2O_5. Water vapor is adsorbed by this deposition when the tube is opened and is only very slowly desorbed again. (II) H_2O is generated by the dissociation of the quartz glass in hot H_2 /6/. (III) The synthetic quartz glass used here ("Suprasil", Heraeus/Hanau) initially contains a very high concentration of ~ 1000 ppm OH, which is dryed out at high temperature. (IV) The solution itself may contain O_2 oxidizing the Si. During the vacuum bake of the In the sources (III) and (IV) are active, and during the bake under H_2 of the complete solution all four sources may play a role.

In order to get an estimate of these effects we have measured the H_2O concentration at the inlet and the outlet of the tube without growth solution at different temperatures and flow rates. At low H_2O concentrations the response time of the sensors, which were calibrated at the actual dew points, is extremely long (3 days at 0.1 ppm_V H_2O). The results are collected in Table I and are interpreted as follows: The value < 0.1 ppm H_2O at the inlet of the tube demonstrates the leak-tightness of the Pd-diffusion cell. At the outlet the H_2O concentrations were found to be inversely proportional to the flow velocity $v(H_2)$, which is expected to be true if initially dry H_2 picks up H_2O molecules from the walls. At a tube used for many growth runs, 1.2 ppm H_2O are found at RT. If the tube is cleaned by HF, this value decreases to 0.2 ppm. This dependence on the etching is attributed to effect (I). The found difference of the H_2O concentrations between T = 20 ^oC and 850 ^oC, namely Δ = 0.5 ppm (Table I), for the etched and the non-etched tube is due to effects (II) and (III). This result indicates that with the theoretical value of 3.7 ppm at 850 ^oC /6/ the H_2O concentration due to dissociation (II) under usual flow conditions is strongly overestimated and that

Table I. H_2O concentration in the H_2 stream with $v(H_2)$ = 0.56 cm/s at different positions in the epitaxial tube

Position of H_2O sensor	$[H_2O]$ (ppm_v)
Inlet of quartz tube:	< 0.1
Outlet of quartz tube:	
Tube with strong P deposition:	
T = 20 °C	1.2
850 °C	1.7
Freshly etched quartz tube:	
20 °C	0.2
850 °C	0.7
At the boat, 660 °C:	$\leq$ 0.2 (estimated)

the natural drying (III) of a "Suprasil" tube after two years of operation is a minor source of H_2O. From the comparison of the values at the inlet and the outlet of the tube we estimate the concentration at the position of the boat at the prebake temperature of 660 °C to be $\leq$ 0.2 ppm H_2O.

The obtained layer purity was independent of the fact, whether the quartz tube had a P deposition or was freshly etched. This indicates that an influence of water vapor backdiffusing from the P deposition to the boat (effect (I)) can be excluded. In conclusion, we obtain very pure layers under dry prebake conditions. An influence of the effects (II) to (IV) cannot be fully excluded, but the H_2O concentrations gene-

rated by the effects (II) and (III) are smaller than believed so far.

Electrical properties of InP

Hall mobility of n-InP

The Hall mobility μ at T = 300 K versus carrier concentration of our n-InP samples is plotted in Fig. 2. All layers were grown on semi-insulating (100)-oriented InP:Fe substrates. Besides a few samples doped with Sn, Te and Ge,

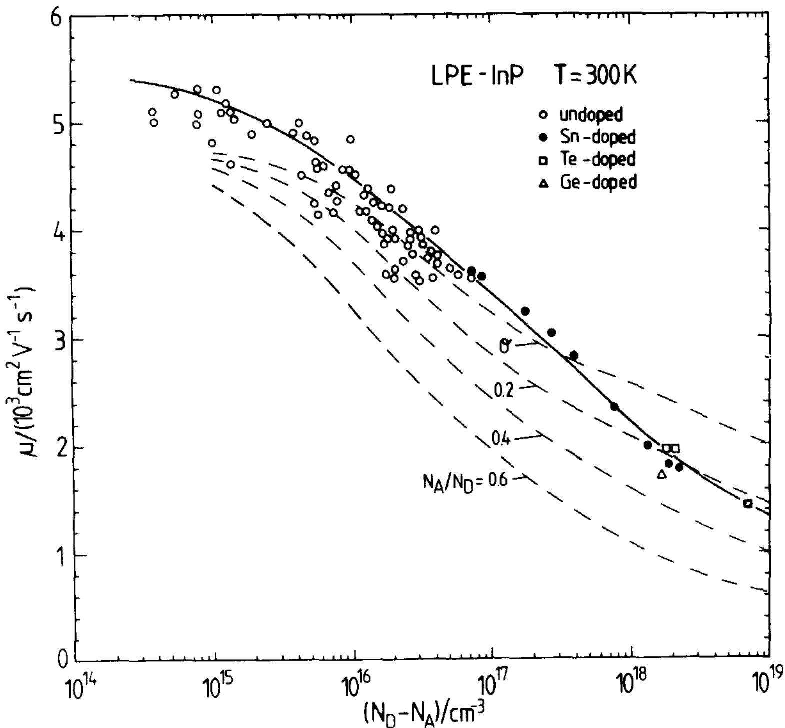

Fig. 2. Hall mobilities at RT of LPE InP layers as a function of carrier concentration. Solid curve: Experimental "universal" mobility curve. Dashed curves: Theoretical drift mobilities after Ref. /14/.

the samples are nominally undoped. The measurement was done by the van der Pauw technique at low electric field strength and at B = 0.5 T. The exact magnetic field strength was calibrated by nuclear magnetic resonance to better than 10^{-3}. Some of the Hall measurements were verified at the RWTH Aachen. The Hall factor r was set equal to one. The figure shows that the μ versus (N_D-N_A) data can essentially be represented by a "universal" curve independent of the doping element. Such a "universal" curve independent of the dopant was previously reported for the case of GaAs by various authors /12, 13/. The dashed curves in the figure represent the theoretical drift mobilities for different compensation ratios N_A/N_D after Walukiewicz et al. /14/. For low N_D-N_A the measured Hall mobilities exceed the curve with $N_A/N_D = 0$, while for high N_D-N_A the data join the curve with $N_A/N_D = 0.2$. This discrepancy can be easily removed, if the drift mobilities $\mu_D = \mu/r$ are compared with the theoretical curves. Following Rode /15/, the Hall factor of pure InP at T = 300 K is $r \approx 1.25$. With increasing carrier concentration r decreases and approaches r = 1 for degenerate material. If these values of r are used, the mobility data yield a compensation ratio $N_A/N_D \approx 0.2$ over the entire doping range between 4×10^{14} and 7×10^{18} cm^{-3}.

In Fig. 3 the mobility data at 77 K of the same samples are plotted and also compared to the theoretical drift mobilities /14/. Here again a "universal" mobility curve independent of the doping element seems to exist. At 77 K the difference between drift- and Hall-mobility is less than 5 % /15/. Therefore, the compensation ratios can be directly derived from a comparison of the Hall data with the dashed curves; they vary between $N_A/N_D = 0.15$ and 0.30. Fair agreement is found with mobility data of LPE n-InP of Cook et al. /9/.

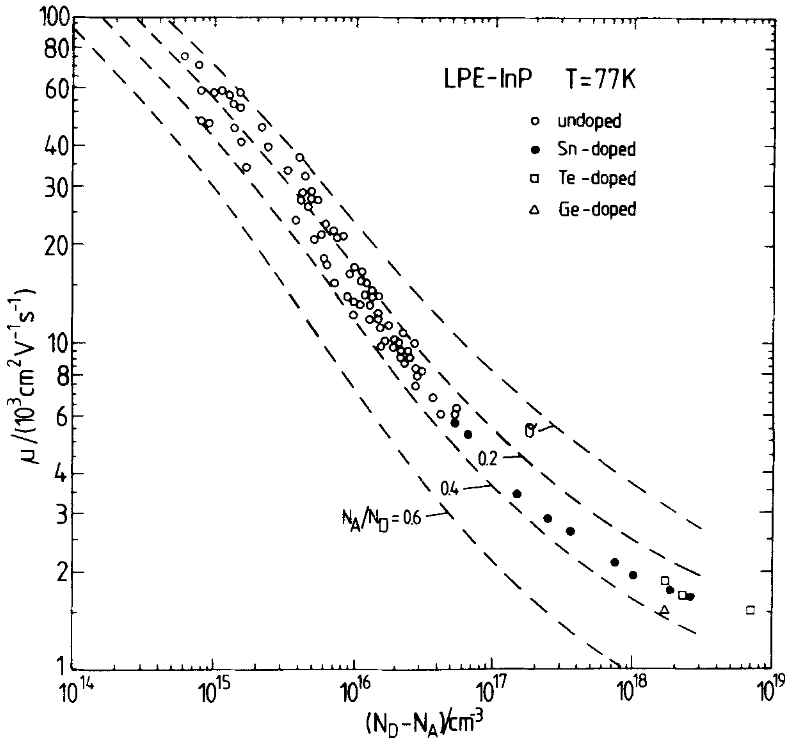

Fig. 3. Hall mobilities at T = 77 K of LPE InP layers as a function of carrier concentration. Dashed curves: Theoretical drift mobilities after Ref. /14/.

The highest purity we have obtained was $N_D-N_A = 4 \times 10^{14}$ cm^{-3}, $\mu(296$ K$) = 5{,}310$ cm^2/Vs and $\mu(77$ K$) = 75{,}000$ cm^2/Vs. These values are among the very best transport data achieved for InP so far.

It has been reported that for unknown reasons contacted high purity InP samples reveal an increase of mobility together with a decrease of carrier concentration when aged over a period of several months /9, 16/. Such a drift could

not be observed even with our purest samples after one year.

Residual carrier concentration as a function of growth temperature

Concerning the problem of the optimum growth temperature of LPE InP and InGaPAs the following arguments can be put forward. The advantages of a high growth temperature ($T_G \geq 650\ ^{\circ}C$) are:

a) Larger layer thicknesses are achieved.

b) Accurate weighing of the components of the growth solution is easier.

c) The miscibility region in the quaternary system is smaller /17/.

d) After Astles et al. /18/ higher purity in undoped InP is obtained at higher growth temperatures. This is in contrast to our results, as will be shown in the following.

The advantages of a low growth temperature ($T_G \leq 600\ ^{\circ}C$) are:

a) Small layer thicknesses can be better controlled.

b) The strain at heterojunctions when cooling down to room temperature is smaller.

c) The compositional grading of InGaAs due to a finite cooling span has a minimum at $T_G = 550\ ^{\circ}C$ /19/.

d) The thermal degradation of the substrate is so small that a meltback of the degraded surface prior to growth or a stabilization by application of P vapor pressure are no longer necessary. We found that the layer morphology is much improved if the layer is grown at low temperature directly on a substrate which was stored under a graphite plug spaced by 50 µm, compared to growth on a substrate which was etched back by an In + InP solution.

e) Under certain conditions InP can be grown on top of InGaAs /20/.

As the advantages of a low T_G dominate, we have examined whether very pure layers can also be grown at low temperatures. Up to now, high purity InP was only achieved at $T_G \geq 650$ °C /6-9/. In Table II the electrical properties of some of our best InP samples are listed as a function of T_G. A residual carrier concentration $N_D - N_A < 10^{15}$ cm^{-3} and high LN_2 mobilities are found independent of the growth temperature in the range between 600 and 650 °C. Thus it is shown, that a reported temperature dependence of the residual carrier concentration /18/ is not of a fundamental nature and that the purity achieved at $T_G \geq 650$ °C /6-9/ can also be

Table II. Electrical characteristics of nominally undoped InP layers as a function of the growth temperature T_G. The (In + InP)-solution was baked in each case for only 15 h at 660 °C under dry H_2.

T_G	$N_D - N_A$/(10^{15} cm^{-3})		μ/(cm^2/Vs)	
(°C)	296 K	77 K	296 K	77 K
650 → 635	1.4	1.4	4,620	45,500
	0.79	0.88	5,080	46,400
635 → 620	1.0	1.2	5,300	57,400
	0.55	0.8	5,230	70,600
	0.79	1.0	5,310	58,400
605 → 590	1.3	1.4	5,170	54,000
	0.51	0.80	4,010	58,200
	1.5	1.6	5,020	53,000
	0.77	1.02	4,960	59,000
	0.37	0.63	5,100	75,000

achieved at 600 °C. Thus, we can take advantage of the above quoted merits of a lower growth temperature. As the solution was held at T_G for only 1 h, but was held at the prebake temperature of 660 °C for 15 h (without substrate) in all cases, it is understandable that the residual carrier concentration essentially depends on the prebake temperature, but not on T_G. The results further indicate that the distribution coefficients of the residual impurities (Si, S) are rather independent of temperature in the range of 600 to 650 °C.

In Table II the carrier concentrations at RT are in most cases smaller than at 77 K. This unphysical result is a consequence of the assumption of the Hall factor r = 1 made in our van der Pauw analysis. This discrepancy is easily removed if $(N_d-N_A) = r(N_D-N_A)_{v.d.P.}$ is used with actual values r(296 K) ≃ 1.25 and r(77 K) ≃ 1.0.

<u>Electrical properties of $In_{0.53}Ga_{0.47}As$</u>

<u>n-$In_{0.53}Ga_{0.47}As$</u>

InGaAs single layers lattice-matched ($\Delta a/a < 10^{-3}$) to s.i. (100)-oriented InP substrates were grown at temperatures between T_G = 495 and 635 °C from (In + InAs + GaAs)-solutions. At T_G = 495 °C lattice-matched growth was possible from a solution consisting of only In + GaAs. At this low temperature the surface of the layer was, however, rough, caused by the miscibility gap in the In-Ga-As system /21/. For $T_G \leq 600$ °C a melt-back of the substrate prior to growth was no longer necessary. Layer thicknesses were between 3 and 12 µm for cooling intervals between 1 and 3 °C and a supersaturation of ~ 7 °C. For the growth of high-purity InGaAs a similar bake procedure was applied as for InP, namely a vacuum bake of the In alone and a bake of the complete solution under dry H_2 at 680 °C in the epitaxial tube.

A bake during 15 h in H_2 routinely yielded a background doping of $n \lesssim 3 \times 10^{15}$ cm^{-3}. Longer bake times up to 65 h yielded best values of $N_D - N_A = 2.5 \times 10^{14}$ cm^{-3}, $\mu(296$ K$) = 12,840$ cm^2/Vs and $\mu(77$ K$) = 53,600$ cm^2/Vs. The growth temperature of these latter samples was $T_G = 630$ °C.

The Hall mobilities versus carrier concentration at RT and T = 77 K of our $In_{0.53}Ga_{0.47}As$ layers are plotted in Fig. 4. For comparison the

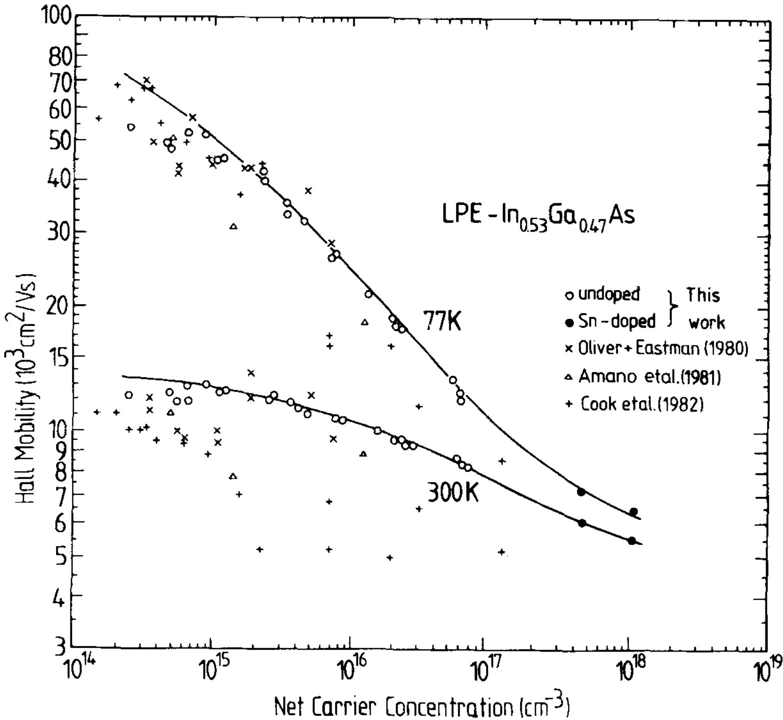

Fig. 4. Hall mobilities at T = 300 K and 77 K of LPE n-$In_{0.53}Ga_{0.47}As$ layers as a function of carrier concentration. Besides the own data the results of Refs. /9, 22, 23/ are included. The solid curves represent averages through the best data.

data of Oliver and Eastman /22/, Amano et al. /23/ and Cook et al. /9/ are also included. At T = 77 K, higher mobilities than ours have already been obtained /9, 22/ for very low doped ($n < 4 \times 10^{15}$ cm^{-3}) material, whereas for higher carrier concentrations the mobilities of this work are consistently higher. At room temperature the very best mobility of Oliver and Eastman is again slightly higher than ours, but their data exhibit a much larger scattering. The RT mobilities of Cook et al. are noticeably lower over the whole carrier concentration range than ours. The solid lines are averaged through the best data and are considered as the actual mobility versus carrier concentration relationships of nearly uncompensated and lattice-matched $In_{0.53}Ga_{0.47}As$. These curves indicate distinctly higher mobilities for a given carrier concentration than those drawn by Cook et al. /9/. A comparison of the RT mobilities of InGaAs with those of GaAs (e.g. Ref. /12/) shows that $\mu(InGaAs)/\mu(GaAs) \simeq 1.7$ over the whole doping range of technical interest between 10^{15} and 10^{18} cm^{-3}, demonstrating the exceptional electrical features of this ternary material.

The photoluminescence properties of our $In_{0.53}Ga_{0.47}As$ can be summarized as follows: At T = 2 K and under very low intensity (< 10 mW/cm^2) laser excitation with $\lambda = 647.1$ nm the PL spectra exhibit an excitonic peak near 0.80 eV of 3.5 meV halfwidth. This value is to be compared with halfwidths of 8 meV /24/ and 2-3 meV /25/ in LPE samples, 4-5 meV /25/ in VPE samples and 5 meV /24/ in MBE samples from other laboratories. The rather large excitonic halfwidth in high-purity mixed crystals is due to random fluctuations of the alloy composition. The only acceptor found in our samples was Zn, but neither the C nor the Si acceptor /25/ could be detected.

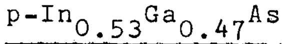

p-$In_{0.53}Ga_{0.47}As$

For the realization of n-channel inversion MISFET's in InGaAs as structure consisting of s.i. InP substrate / p^--InP buffer layer / p^--InGaAs channel layer / n^+-InGaAs contact layer is utilized /4/. The problem of this structure is to generate a p^--layer doped as low as possible. The lower the p-doping, the higher is the inversion mobility.

The doping element used here was Zn. As the distribution coefficient of Zn is very large, in the initial experiments the dopant was added as a ZnIn alloy. For this purpose five different ZnIn alloys were prepared by melting In and Zn in an evacuated ampoule at 900 °C, which contained 0.05, 0.5, 1.8, 2.8 and 4 wt.% Zn, respectively. By energy dispersive analysis of x-rays (EDX) in a SEM it was found that Zn was homogeneously distributed only in the alloy with 1.8 wt.% Zn. In all other alloys local precipitations of Zn and areas without Zn were found. Those alloys are, therefore, not suitable as a dopant. The x-ray analysis indicates that the eutectic composition of ZnIn is

$$\text{ZnIn(eut.)} \hat{=} 1.8 \text{ wt.\% Zn.} \qquad (1)$$

Reported values for the eutectic composition are between 1.8 and 4.75 wt.% Zn /26/. With our eutectic alloy reproducible doping of InGaAs could be achieved for $p > 10^{17}$ cm^{-3}. To minimize evaporation loss of Zn, the piece of ZnIn was put under the prebaked solution, and the bin was capped by a graphite cover.

In order to obtain hole concentrations in InGaAs over the whole range from some 10^{15} cm^{-3} to 10^{18} cm^{-3}, we have applied a novel technique: Doping was accomplished by the use of Zn-doped GaAs. As the required quantity of GaAs in the (In + GaAs + InAs)-solution is fixed by the condition of lattice-matching, the amount of GaAs was composed of undoped and Zn-doped monocrystalline GaAs to obtain the desired Zn con-

centration in InGaAs. A further variation of the Zn concentration in InGaAs was enabled by the use of differently Zn-doped GaAs (N_A-N_D = 1 x 10^{18} cm^{-3} and 6 x 10^{19} cm^{-3}).

Using this doping technique, hole concentrations in $In_{0.53}Ga_{0.47}As$ down to

N_A-N_D = 5.5 x 10^{15} cm^{-3} could be produced for the first time, as is depicted in Fig. 5. As a necessary condition the n-type background doping

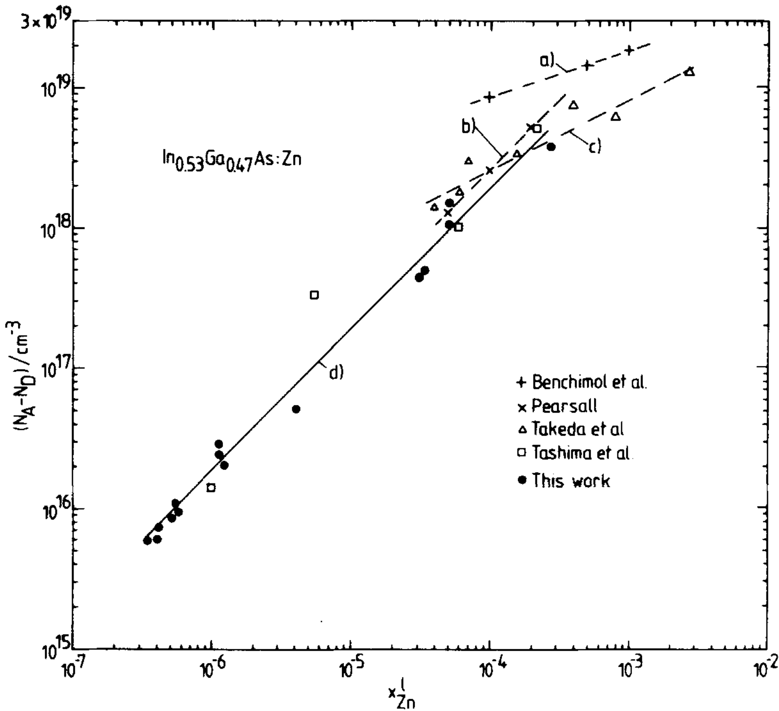

Fig. 5. Hole concentration at RT of LPE p-$In_{0.53}Ga_{0.47}As$ layers as a function of the atomic fraction of Zn in the liquid. Besides the own data the results of Refs. /28-31/ are included. The straight lines a) to d) represent averages through the respective sets of data.

must be sufficiently small (N_D-N_A $\leq$ 3 x 10^{15} cm^{-3}). If the Zn concentration in the liquid was x^l_{Zn} < 2 x 10^{-7}, the resultant layer became n-type. In these experiments the growth solution except the GaAs:Zn was prebaked for 15 h, and the GaAs:Zn was added when the substrate was loaded. The growth temperature was 595 °C. This doping technique is highly reproducible ($\pm$ 10 %), as is seen from Fig. 5. This reproducibility cannot be achieved with ZnIn as a dopant. The highest hole concentration obtained with GaAs:Zn doping was N_A-N_D = 1.5 x 10^{18} cm^{-3}. The carrier concentration was here determined by C-V-measurements at the p-n^+ junction in InGaAs in the above mentioned MISFET structures.

The relation between N_A-N_D and x^l_{Zn} after Fig. 5 is linear for N_A-N_D $\leq$ 3 x 10^{18} cm^{-3} and reads

$$\frac{N_A - N_D}{cm^{-3}} = (1.9 \pm 0.2)\ 10^{22}\ x^l_{Zn}. \qquad (2)$$

The resultant distribution coefficient is

$$k_{Zn} = 0.65 \pm 0.07, \qquad (3)$$

where Eq. 2 of Ref. /27/ and $\rho(In_{0.53}Ga_{0.47}As)$ = 5.532 g/cm^3 were used.

In Fig. 5 all published data known to us of Zn-doped $In_{0.53}Ga_{0.47}As$ are also included. These are results of Tashima et al. /28/ (T_G = 628 °C) and in the range of high doping results of Benchimol et al. /29/ (T_G ≈ 625 °C), of Pearsall /30/ (T_G = 620 °C) and of Takeda et al. /31/ (T_G = 650 °C). Except for the data of Benchimol et al. all results are in fair agreement with each other. The slopes of the N_A-N_D versus x^l_{Zn} curves are 0.32 (Benchimol), 0.50 (Takeda) and 1.0 (Pearsall, Tashima, and ours), respectively. Combining all data, we can conclude that N_A-N_D is proportional to x^l_{Zn} in the range x^l_{Zn} $\leq$ 2 x 10^{-4}, but for higher Zn concentrations approaches a saturation value near 2 x 10^{19} cm^{-3}.

Conclusion

It has been demonstrated that InP and $In_{0.53}Ga_{0.47}As$ layers which have net carrier concentrations in the 10^{14} cm^{-3} range can be grown by LPE using a time saving bakeout procedure. For given source materials the achievable layer purity is determined by the quality of the individual quartz tube and H_2 supply rather than by the graphite boat. The growth temperature could be lowered without loss of layer purity to 600 °C. This enabled us to avoid the melt-back step with the further advantage of a considerably improved layer morphology. Low-doped p-InGaAs could be grown with good reproducibility by applying a novel doping technique, where GaAs:Zn is the doping source. Using these epitaxial layers ternary pin photodetectors with extremely low dark current density /2/ and ternary MISFET's with high field effect mobility /4/ have been realized.

Acknowledgement

The authors would like to thank H. Westenberger and K. Orth for their valuable assistance in growing the layers, A. Pöcker for the EDX and the x-ray diffraction measurements, and K.H. Goetz (RWTH Aachen) for the PL measurements.

References

/1/ S.R. Forrest, IEEE J. Quantum Electron. QE-17, 217 (1981).

/2/ H. Nickel and E. Kuphal, J. Opt. Commun., in press.

/3/ A.S.H. Liao, B. Tell, R.F. Leheny, and T.Y. Chang, Appl. Phys. Lett. 41, 280 (1982).

/4/ D. Fritzsche, E. Kuphal, and G. Weimann, Proc. Int. Conf. Solid State Devices, Tokyo (1982), Suppl. of Jpn. J. Appl. Phys.

/5/ E. Kuphal and A. Pöcker, J. Cryst. Growth 58, 133 (1982).

/6/ V.L. Wrick, K.T. Ip, and L.F. Eastman, J. Electron. Mater. 7, 253 (1978).

/7/ S.H. Groves and M.C. Plonko, Inst. Phys. Conf. Ser. No. 45, 71 (1979).

/8/ D.E. Holmes and G.S. Kamath, J. Cryst. Growth 54, 51 (1981).

/9/ L.W. Cook, M.M. Tashima, N. Tabatabaie, T.S. Low and G.E. Stillman, J. Cryst. Growth 56, 475 (1982).

/10/ S.H. Chiao and G.A. Antypas, J. Appl. Phys. 49, 466 (1978).

/11/ E. Kuphal, Res. Inst. German Post Office, Tech. Rept. 65 TBr 20, part I (1979).

/12/ E. Kuphal, A. Schlachetzki, and A. Pöcker, Appl. Phys. 17, 63 (1978).

/13/ H. Poth, H. Bruch, M. Heyen, and P. Balk, J. Appl. Phys. 49, 285 (1978).

/14/ W. Walukiewicz, J. Lagowski, L. Jastrzebski, P. Rava, M. Lichtensteiger, C.H. Gatos, and H.C. Gatos, J. Appl. Phys. 51, 2659 (1980).

[illegible] [illegible], Phys. Status Solidi B 55, 687 (1973).

[illegible] [illegible] Eastman, in Proc. 1980 NATO Sponsored [illegible] Workshop (1980) p. 117.

[illegible] [illegible], Jpn. J. Appl. Phys. 21, 797 (1982).

/18/ M.C. Astles, F.G.H. Smith, and E.W. Williams, J. Electrochem. Soc. 120, 1750 (1973).

/19/ A.R. Clawson, NOSC Technical Note 772 (1979).

/20/ K. Nakajima, S. Yamazaki, and K. Akita, Jpn. J. Appl. Phys. 21, L237 (1982).

/21/ E. Kuphal, Res. Inst. German Post Office, Tech. Rept. 65 TBr 20, part III (1983).

/22/ J.D. Oliver, Jr. and L.F. Eastman, J. Elctron. Mater. 9, 693 (1980).

/23/ T. Amano, K. Takahei, and H. Nagai, Jpn. J. Appl. Phys. 20, 2105 (1981).

/24/ H. Ohno, C.E.C. Wood, L. Rathbun, D.V. Morgan, G.W. Wicks, and L.F. Eastman, J. Appl. Phys. 52, 4033 (1981).

/25/ K.H. Goetz, A.V. Solomonov, D. Bimberg, H. Jürgensen, M. Razeghi, J. Selders, subm. to J. Appl. Phys.

/26/ M. Hansen, "Constitution of binary alloys". McGraw-Hill Book Company, Inc. (1958).

/27/ E. Kuphal, J. Cryst. Growth 54, 117 (1981).

/28/ M.M. Tashima, L.W. Cook, and G.E. Stillman, Appl. Phys. Lett. 39, 960 (1981).

/29/ J.L. Benchimol, M. Quillec, C. LeCornec and G. LeRoux, Appl. Phys. Lett. 36, 454 (1980).

/30/ T.P. Pearsall, IEEE J. Quantum Electron. QE-16, 709 (1980).

/31/ Y. Takeda, M. Kuzuhara, and A. Sasaki, Jpn. J. Appl. Phys. 19, 899 (1980).